ISSN 1063-7729, Astronomy Reports, 2007, Vol. 51, No. 9, pp. 773–779. © Pleiades Publishing, Ltd., 2007.
Original Russian Text © N.I. Kobanov, A.A. Sklyar, 2007, published in Astronomicheskiĭ Zhurnal, 2007, Vol. 84, No. 9, pp. 857–864.

Periodic Processes and Plasma Motions in Solar Coronal Holes

N. I. Kobanov and A. A. Sklyar

Institute of Solar-Terrestrial Physics, Siberian Division, Russian Academy of Sciences, P.O. Box 4, Irkutsk, 664033 Russia

Received April 4, 2007; in final form, April 5, 2007

Abstract—Episodic observations of coronal holes were carried out simultaneously in several spectral lines during the 2002–2005 observational seasons. An analysis of eighteen time series is used to obtain the amplitude–spectral properties of oscillatory wave motions of the solar plasma at the bases of coronal holes. It is found that the amplitudes of the 5-min and 3-min line-of-sight velocity oscillations increase in coronal holes. Low-frequency (1–2 mHz) oscillations are concentrated at the boundaries of the chromospheric network, while the 3-mHz and 5-mHz oscillations dominate in the network cells. Clear indications of propagating waves have been found at the bases of coronal holes. The 3 mHz phase velocities are 45 ± 5 km/s and 80–100 km/s for the equatorial and polar coronal holes, respectively.

PACS numbers: 96.60.pc, 95.85.Kr, 96.60.Ly
DOI: 10.1134/S1063772907090077

1. INTRODUCTION

Coronal holes were first detected by spacecraft X-ray observations in the latter half of the 20th century. Optical studies of coronal holes have since been carried out extensively at wavelengths from the extreme ultraviolet to the near infrared. Analyses of their radio emission has also brought a number of interesting findings [1, 2]. For example, some changes in the radio radius of the Sun, attributed to limb coronal holes, were noted in [1]. It is generally agreed that a coronal hole (CH) is an open magnetic-field configuration in the solar atmosphere [3]. Observations indicate that the solar wind originates from these holes [4]. The low-speed component of the solar wind is associated with central regions and the high-speed component with the boundary regions of coronal holes [5, 6]. The photospheric magnetic fields in coronal holes have been studied intensely [7–9]. Some authors [10, 11] have noted that magnetic structures in coronal holes evolve much more slowly than those in other unperturbed regions of the solar atmosphere located beyond coronal holes. It has also been argued that coronal holes indicate the presence of large-scale solar magnetic fields, and that the CH dynamics describe the behavior of these fields at the coronal level [7]. The differences between the physical conditions in coronal holes and in the surrounding medium have been intensely studied in recent years [12, 13]. It is quite natural that such differences must be searched for at the bases of coronal holes, in the chromosphere and photosphere [14].

It is well known that solar oscillations are very sensitive to the basic physical conditions: the temperature, density, and strength and configuration of the magnetic field. These last two quantities determine the frequency, wavelength, and propagation velocity, and also the type of oscillations excited. A number of works have considered theories for the excitation and propagation of waves in coronal holes [15]. We hope that studying oscillations inside coronal holes and comparing these with the surrounding atmosphere will help us to understand the contribution of coronal holes to energy transport and exchange in the Sun. For example, do coronal holes play the role of safety valves in the total heating of the corona?

Studies of oscillatory-wave processes in coronal holes have been carried out over a broad range of wavelengths. In particular, Hα observations of coronal holes [16] appear to have detected Moreton waves. Spacecraft observations [17] have enabled investigation of the CH oscillations in the UV as well. Repeating explosive CH events have been explained as an effect of the reconnection of oscillating magnetic tubes of opposite polarities [18].

The purpose of the current work is to extend our understanding of oscillatory processes occurring at the bases of coronal holes by analyzing new observations using various modern facilities, and comparing the results obtained with those obtained previously. This work was carried out as part of a broader research program concerned with oscillations occurring in solar elements with various magnetic-field topologies.

Brief description of observational data

№	Location on the disk	Date and time (UT)	Spectral lines λ, Å	Period, min	
				Photosphere	Chromosphere
1	50°N 0°W	11.09.02 08:02–08:45	Hα, FeI 6569	5, 8	3, 5, 12, 20
2	48°S 15°W	11.09.02 08:55–09:36	Hα, FeI 6569	5	3, 5, 12–15
3	0°S 20°W	16.05.03 03:19–04:51	Hα, FeI 6569	5, 19	3, 5, 9–20
4	5°S 30°W	17.05.03 08:55–09:55	Hα, FeI 6569	5	3, 5, 12, 16, 25
5	40°S 0°W	01.07.03 08:02–09:27	Hα, FeI 6569	5, 19, 22	3, 5, 14–23
6	25°S 27°W	22.05.04 03:22–04:21	BaII 4554, FeI 4551.6	7, 9, 14, 19	
7	25°S 27°W	22.05.04 04:25–05:24	BaII 4554, FeI 4551.6	3, 6, 15, 20	
8	5°S 13°W	28.06.04 02:05–04:12	Hα, FeI 6569	5, 20	3, 5, 9–16, 25
9	80°N 0°W	15.07.05 09:37–10:20	Hα, FeI 6569	5, 10	3, 11
10	0°S 5°W	18.07.05 09:37–10:20	BaII 4554	5, 11	
11	0°S 18°W	19.07.05 03:56–05:00	FeI 5576, CaI 5582	5, 12	
12	0°S 18°W	19.07.05 05:20–06:05	BaII 4554	5, 13	
13	48°N 5°E	04.08.05 04:47–06:17	Hα, FeI 6569	5, 25	3, 5, 15
14	32°S 4°W	04.08.05 06:26–07:09	Hα, FeI 6569	5, 10, 22	3, 5, 15
15	4°N 47°E	11.08.05 02:54–03:51	CaII 8542		3, 5, 15, 25
16	60°N 1°E	11.08.05 04:20–05:00	CaII 8542		3, 5, 14
17	0°N 36°W	17.08.05 05:20–06:43	BaII 4554, FeI 4551.6	5, 11	
18	0°N 37°W	17.08.05 06:58–08:38	CaII 8542	5, 20	5, 11, 20

2. INSTRUMENTS AND TECHNIQUES

We carried out our observations at the Sayan Observatory using the observatory's horizontal solar telescope equipped with a photoelectric servo system enabling image scanning and guiding with an accuracy of 1″. The theoretical spatial resolution of the telescope with its main mirror diameter of 800 mm can reach 0.2″. We used a Princeton Instruments RTE/CCD 256H array (256 × 1024 pixels with a pixel size of 24 mcm). The array is equipped with a thermoelectric cooling system and controller that provides automatic temperature control, facilitating higher sensitivity due to the lower thermal noise. Monitoring of the observations and image recording were provided by the WinSpec32 software. The observations were unmodulated [19] and carried out simultaneously for several spectral lines emitted from two different altitudes, corresponding to the photosphere and chromosphere or the photosphere and temperature minimum. We used the Hα 6562.8 Å, FeI 6569.2 Å, CaII 8542 Å, and BaII 4554 Åspectral lines.

We use eighteen temporal data series on coronal holes with different locations on the disk (both near the equator and at the poles). The table presents a brief description of the data. Each time series is a sequence of images obtained within a single time interval (from 1 to 10 s) with a single exposure. The duration of the series varies from 40 to 125 min. The size of the observed region is determined by the width of the entrance slit and the height of the array along the slit, and was 1.5″ × 60″, on average. Because of atmospheric noise, the spatial resolution during an hour rarely exceeded 1″, and the redundant array resolution (256 pixels per 60″) was reduced by averaging over four neighboring pixels, providing a final resolution of about 1″. In addition, specialized software recorded only the necessary spectral regions,

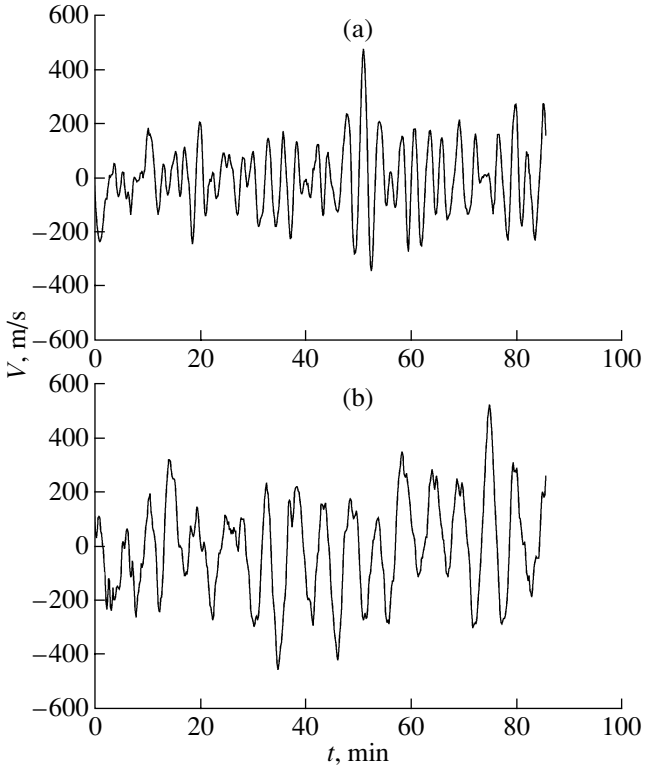

Fig. 1. Fragments of the line-of-sight velocity observed at the base of a coronal hole in the (a) chromosphere and (b) photosphere.

instead of the entire spectrum detected by the array. This significantly reduced the volume of initial data and accelerated the initial processing. We detected the locations of the coronal holes using ultraviolet SOHO images and SOLIS (Synoptic Optical Long-Term Investigations of the Sun) data.

The observational data we used form a long time series obtained simultaneously in the photospheric and chromospheric lines, with the sampling rate reaching two images per second. The data reduction included processing in the IDL package and a wavelet analysis. In our opinion, a wavelet analysis is the most appropriate technique for analyzing wave-train oscillations, and precisely this type of velocity and brightness oscillation dominates in coronal holes. Compared to other spectral methods, wavelet analyses are more convenient for studying the spectral dynamics.

3. RESULTS AND DISCUSSION

At the CH bases, we first examine the five-minute oscillations that dominate in the solar photosphere. The table presents the periods of the CH line-of-sight velocity oscillations observed in the photosphere and chromosphere.

Figure 1 presents some examples of the time series for the line-of sight velocity signals. We did not find any regular decrease in the amplitudes of the CH line-of-sight velocity oscillations, in good agreement with [20, 21], though such a decrease has been detected by other researchers [22]. Initially, we suggested this could be due to differences in the physical conditions in the coronal holes (for mid-disk and polar coronal holes), although the effects of local structures could be even more important. At the photospheric level, these local structures result from supergranulation, mesogranulation, and dark strips between granules, while the local structures above the photosphere are elements of the chromospheric network. The Hα observations clearly trace the chromospheric network structures in the coronal holes. The time-averaged intensity distributions reveal light and dark regions (network cells and network boundaries). The oscillation power distributions become more complex when their relation to spatial structures is taken into account. Nevertheless, we can state with certainty that, on the whole, the amplitudes of the 5-min line-of-sight velocity oscillations increase in coronal holes.

There are more distinct differences between the spectra of the oscillations occurring in different elements of the chromospheric network. The power spectra shown in Fig. 2 display a clear tendency for

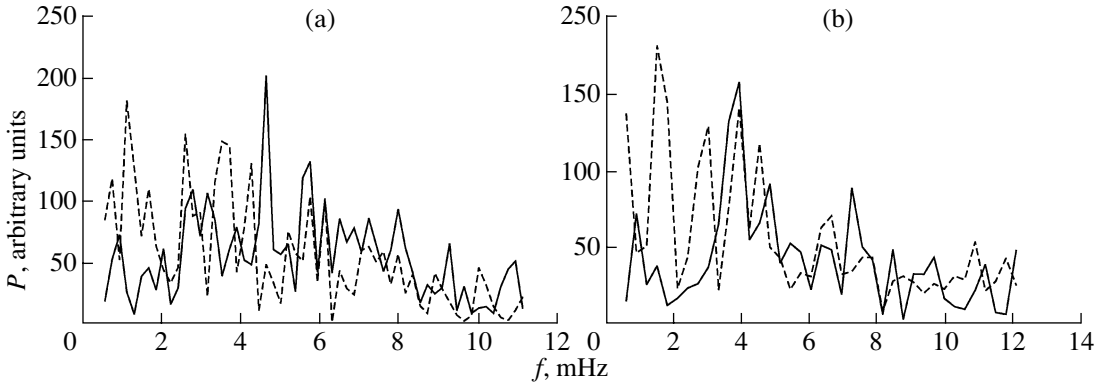

Fig. 2. Oscillation spectra determined for the CH network elements from time series (a) No. 12 and (b) No. 3. The solid and dashed curves show the power spectra for the oscillations inside the cell and at the network boundaries, respectively.

stronger contributions of low-frequency modes at the network boundaries. The wavelet diagram (Fig. 3) describing the spatial distribution of the oscillations of various frequencies also supports this conclusion. Periods of 5–8 and even 10–15 min are detected at the boundaries, while 3–5 min oscillations dominate in the network chromosphere. Recent studies have also revealed this effect for some higher layers. For example, 85 GHz radio observations have shown a difference between the oscillation spectra of different network elements. Namely, the 3-min period dominates inside the cells, and the 5-min oscillations at the network boundaries [23]. It is interesting that the table shows that 10–15 min periods are encountered fairly often. Some researchers [24] have suggested that periods of about 10 min are most probable for the parametric excitation of oscillations at the bases of coronal loops.

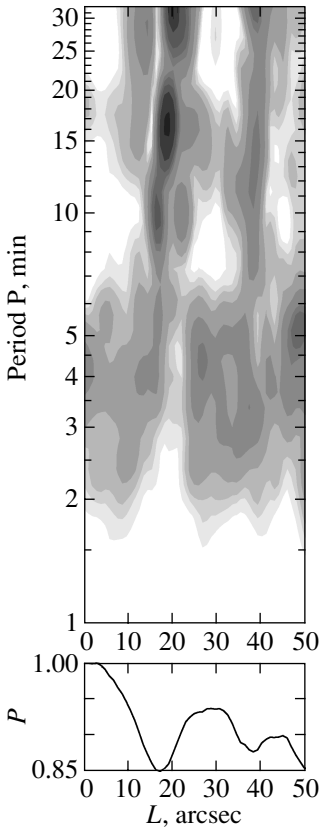

Fig. 3. Wavelet diagram describing the spatial localization of the low-frequency oscillations.

Examining the spatial distribution of quasi-stationary flows, we find that ascending streams, corresponding to blue-shifted spectral lines, are more frequently observed near boundaries of the chromospheric network than inside the network (Fig. 4). This is consistent with our earlier results [20, 21], and is supported by recent studies of the lower corona [25]. Note that accurate estimates require longer time series, in order to eliminate the influence of periodic components.

Distinguishing propagating waves represents a separate problem. Let us suppose that an acoustic wave propagates vertically upwards in a cylindrical volume in a direction coincident with the line of sight and the cylinder axis. In this case, observations at a single altitude (in a single spectral line) cannot distinguish between standing waves and propagating waves. Only observations at several different altitudes can detect the phase delays occurring in propagating waves. However, when the propagation speed is high and the interval of altitudes is small, the phase delay becomes almost unresolved. A wave propagating horizontally or in a hemisphere provides a quite different situation. We can distinguish such a wave through observations in a single spectral line. However, we must take into account the fact that we cannot detect a purely acoustic wave propagating perpendicular to the line of sight via the Doppler effect, but can detect a propagating wave from its

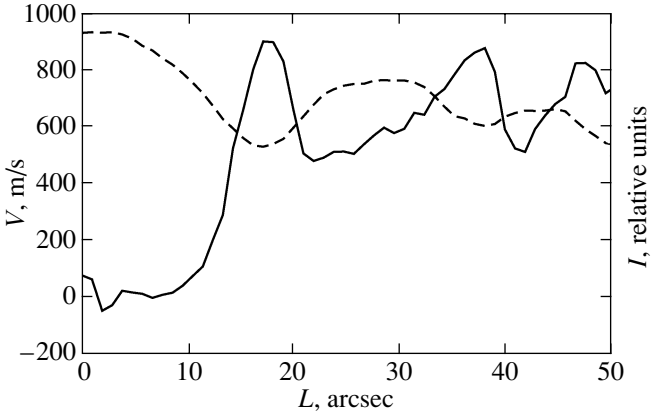

Fig. 4. Ascending streams at low Hα intensities. The solid and dashed curves show the line-of-sight velocity and intensity.

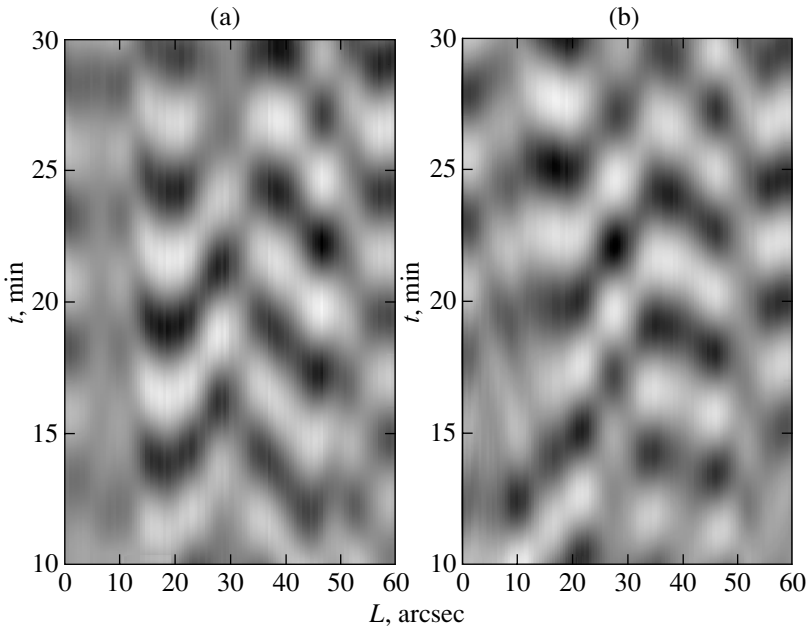

Fig. 5. The 5-min wave propagation in the (a) photosphere and (b) chromosphere according to time series No. 14.

intensities. On the contrary, we can detect horizontal ("kink" or "sausage") Alfven waves from their line-of-sight velocity. Thus, determining the type of wave observed is a rather complex experimental problem, and researchers usually do not attempt to solve this problem simply by making general assumptions.

The "herringbone" structures in spatial–temporal half-tone diagrams of the line-of-sight velocity are good indicators for propagating waves [26]. Our own experience acquired in working with such diagrams indicates that frequency filtering using direct and inverse Fourier transforms is necessary for the reliable detection of propagating waves. In this case, we construct individual half-tone diagrams for each frequency used. To determine the frequency components for the frequency filtering, we use wavelet diagrams or power spectra averaged over the spatial coordinate. In all half-tone line-of-sight velocity diagrams, dark and light areas indicate velocities directed away from and toward the observer.

Our analysis of diagrams of this kind for coronal holes sometimes shows clear indications of herringbone structures. Figure 5a presents a segment of a diagram that undoubtedly indicates a propagating wave process observed in the photosphere beneath a coronal hole. The horizontal projection of the propagation velocity determined by the inclination of the herringbones reaches 45 ± 5 km/s. The next question

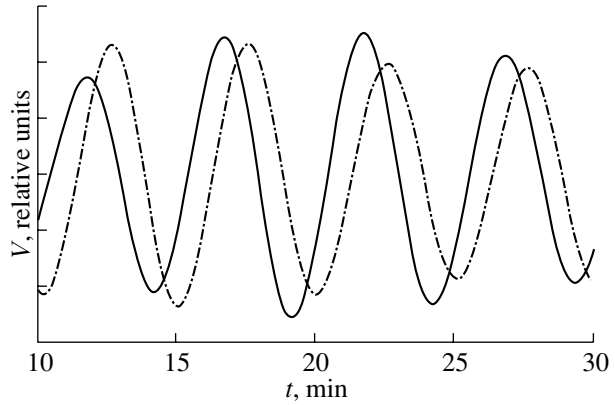

Fig. 6. The chromospheric delay for the line-of-sight velocity corresponding to the point $L = 21''$ in Fig. 5.

is the corresponding process in the chromosphere. Unfortunately, the herringbone structures in the halftone Hα line-of-sight velocity diagrams (Fig. 5b) are not as distinct as those in the photosphere. Nevertheless, there are some indications of a propagating wave in these diagrams. These clearly demonstrate that we have observed a propagating wave process in the lowest layers of a coronal hole.

The graphical image of the photospheric and chromospheric line-of-sight velocity signals above the point ($21''$) indicates a 40–50 s delay for the chromospheric signal (Fig. 6). Assuming an altitude distance of 1500–2000 km, we obtain a propagation velocity of 40–45 km/s for the chromosphere. This velocity corresponds to mid-latitude coronal holes, while the velocity in polar coronal holes reaches 80–100 km/s. Although our estimate for the altitude distance may be incorrect for limb observations, it is reasonable to compare our results with spacecraft observations for higher altitudes. It was found by analyzing oscillations in the transition region and lower corona that the 10-min oscillations propagated upwards with phase velocities of 54 km/s for equatorial and 89 km/s for polar coronal holes [27]. Propagating oscillations were more frequently observed at the boundaries of the chromospheric network [28]. We do not have a sufficient number of observations with distinct propagating waves to firmly draw this conclusion, however, especially for polar coronal holes.

4. CONCLUSIONS

Oscillation processes are not suppressed inside coronal holes at the photospheric–chromospheric level, as is demonstrated by the 3–5-min oscillations, whose amplitudes are frequently increased in coronal holes compared to the surrounding medium.

The various elements of the chromospheric network exert a selective influence on oscillations of different frequencies. Low-frequency oscillations (1–2 mHz) are concentrated at the network boundaries, while 3- and 5-min oscillations dominate in the network cells. Quasi-stationary ascending streams are also more frequently observed at the network boundaries.

We have found clear indications of propagating waves at the bases of coronal holes. The 3 mHz phase velocity reaches 45 ± 5 km/s for equatorial and 80–100 km/s for polar coronal holes.

ACKNOWLEDGMENTS

This work was supported by the Russian Foundation for Basic Research (project code 05-02-16325), the Program for Leading Scientific Schools of the Russian Foundation (NSh 4741.2006.2), and the Basic Research Program of the Presidium of Russian Academy of Sciences (P-16).

REFERENCES

1. V. N. Borovik and M. A. Livshits, Astron. Zh. **59**, 355 (1982) [Sov. Astron. **26**, 215 (1982)].
2. V. N. Borovik, M. Sh. Kurbanov, M. A. Livshits, and B. I. Ryabov, Astron. Zh. **70**, 403 (1993) [Astron. Rep. **37**, 208 (1993)].
3. J. B. Zirker, *Coronal Holes and High-Speed Wind Streams* (Colorado Associated Univ. Press, 1977).
4. S. R. Cranmer, Space Sci. Revs **101**, 229 (2002).
5. L. M. Kozlova and B. V. Somov, Astron. Zh. **77**, 63 (2000) [Astron. Rep. **44**, 401 (2000)].
6. S. Robbins, G. J. Henney, and J. W. Harvey, Sol. Phys. **233**, 265 (2006).
7. V. N. Obridko and B. D. Shelting, Sol. Phys. **124**, 73 (1989).
8. E. I. Mogilevsky, V. N. Obridko, and N. S. Shilova, Sol. Phys. **176**, 107 (1997).
9. N. Meunier, Astron. Astrophys. **443**, 309 (2005).
10. V. I. Abramenko, L. A. Fisk, and V. B. Yurchyshyn, Astrophys. J. **641**, L65 (2006).
12. J. Zhang, J. Ma, and H. Wang, Astrophys. J. **649**, 464 (2006).
12. K. Bocchialini and J. C. Vial, Sol. Phys. **168**, 37 (1996).
13. K. Wilhelm, Astron. Astrophys. **455**, 697 (2006).
14. R. B. Teplitskaya, O. A. Ozhogina, and I. P. Turova, Pis'ma Astron. Zh. **32**, 133 (2006) [Astron. Rep. **32**, 120 (2006)].
15. B. N. Dwivedi and A. K. Srivastava, Sol. Phys. **237**, 143 (2006).
16. A. M. Veronig, M. Temmer, B. Vrsnak, and J. K. Thalmann, Astrophys. J. **647**, 1466 (2006).
17. S. W. McIntosh, B. Fleck, and T. D. Tarbell, Astrophys. J. **609**, L95 (2006).
18. J. G. Doyle, M. D. Popescu, and Y. Taroyan, Astron. Astrophys. **446**, 327 (2006).

19. N. I. Kobanov, Prib. Tekh. Eksp. №. 4, 110 (2001) [Instrum. Exp. Tech., №. 4, ? (2001)].
20. N. I. Kobanov and D. V. Makarchik, Astron. Zh. **80**, 1026 (2003) [Astron. Rep. **47**, 946 (2003)].
21. N. I. Kobanov, D. V. Makarchik, and A. A. Sklyar, Sol. Phys. **217**, 53 (2003).
22. E. V. Malanushenko, V. P. Malanushenko, and N. N. Stepanian, in *Motions in Solar Atmosphere*, Ed. by A. Hanslmeier and M. Messerotti (Kluwer Acad. Press, Astrophys. Space Sci. Lib., 1999), Vol. 239, p. 251.
23. S. M. White, M. Loukitcheva, and S. K. Solanki, Astron. Astrophys. **456**, 697 (2006).
24. V. V. Zaitsev and A. G. Kislyakov, Astron. Zh. **83**, 921 (2006) [Astron. Rep. **50**, 823 (2006)].
26. T. Aiouaz, H. Peter, and P. Lemaire, in *Coronal Heating. Proceedings ot the SOHO 15 Workshop*, ESA SP-575 (ESA, 2004), p. 331.
26. N. I. Kobanov, D. Y. Kolobov, and D. V. Makarchik, Sol. Phys. **238**, 231 (2006).
27. D. Banerjee, E. O'Shea, and J. G. Doyle, in *Chromospheric and Coronal Magnetic Fields*, ESA SP-596 (ESA, 2005), p. 41.
28. M. D. Popescu, L. D. Xia, and J. G. Doyle, in *Coronal Heating. Proceedings ot the SOHO 15 Workshop*, ESA SP-575 (ESA, 2004), p. 513.

Translated by V. Badin